GA–A26393

ALPHA PARTICLE DIAGNOSTICS AND PHYSICS STUDIES

FINAL REPORT TO THE
U.S. DEPARTMENT OF ENERGY
for the period
MARCH 1, 2007 through FEBRUARY 28, 2009

by
R.K. FISHER

DATE PUBLISHED: MAY 2009

GENERAL ATOMICS

DISCLAIMER

GA–A26393

ALPHA PARTICLE DIAGNOSTICS AND PHYSICS STUDIES

FINAL REPORT TO THE
U.S. DEPARTMENT OF ENERGY
for the period
MARCH 1, 2007 through FEBRUARY 28, 2009

by
R.K. FISHER

Work supported by the
Department of Energy under
DE-FG02-92ER54150

GENERAL ATOMICS PROJECT 03937
DATE PUBLISHED: MAY 2009

GENERAL ATOMICS

1. INTRODUCTION

The study of burning plasmas is the next frontier in fusion energy research, and will be a major objective of the U.S. fusion program through U.S. collaboration with our international partners on the ITER Project. For DT magnetic fusion to be useful for energy production, it is essential that the energetic alpha particles produced by the fusion reactions be confined long enough to deposit a significant fraction of their initial ~ 3.5 MeV energy in the plasma before they are lost. Development of diagnostics to study the behavior of energetic confined alpha particles is a very important if not essential part of burning plasma research. Despite the clear need for these measurements, development of diagnostics to study confined the fast confined alphas to date has proven extremely difficult, and the available techniques remain for the most part unproven and with significant uncertainties.

Research under this grant had the goal of developing diagnostics of fast confined alphas, primarily based on measurements of the neutron and ion tails resulting from alpha particle knock-on collisions with the plasma deuterium and tritium fuel ions. One of the strengths of this approach is the ability to measure the alphas in the hot plasma core where the interesting ignition physics will occur.

1.1. 2007–2009 PRESENTATIONS, PUBLICATIONS

"Novel Applications of Neutron Activation Techniques on ITER," R.K. Fisher, presented at 2008 APS HTPD Conference in Albuquerque, NM

"Alpha Knock-On Measurements on ITER Using Neutron Activation," R.K. Fisher, presented at 12th ITPA Topical Group Meeting on Diagnostics, March 26 to April 1, 2007, Princeton, NJ

"Novel Applications of Neutron Activation Techniques on ITER," R.K. Fisher, paper to be submitted to *Plasma Physics and Controlled Fusion* or possibly *Review of Scientific Instruments* (February–March 2009).

1.2. PROGRESS DURING THE PAST GRANT YEAR

Research under this grant has concentrated on using threshold activation reactions to measuring the alpha knock-on neutron tail in ITER. Significant progress has been made in this area, and Section 2 of this final report is based on a draft of a paper planned for submission to either *Plasma Physics and Controlled Fusion* or possibly *Review of Scientific Instruments* that describes the results of this research.

2. NOVEL APPLICATIONS OF NEUTRON ACTIVATION TECHNIQUES ON ITER

2.1. ABSTRACT

Novel applications of neutron activation techniques are proposed to aid in the measurements of the total DT neutron production, the spatial profile of the neutron emission, and the energetic neutrons above ~ 16 MeV resulting from DT alpha particle collisions with fuel ions on ITER.

2.2. INTRODUCTION

The ITER experiment is designed to demonstrate the scientific and technological feasibility of energy production using magnetic fusion. ITER is designed to produce significant fusion power ~ 500 MW for 300–500 s, and will be the first experiment capable of producing a burning deuterium-tritium plasma, where the majority of the plasma heating needed to sustain the fusion reactions will be provided by the fusion-generated alpha particles. The neutron power load on the first wall will be > 0.5 MW-m^{-2}, equivalent to >2•10^{13} n-cm^{-2}-s^{-1} of incident 14 MeV neutrons. Designed to produce a neutron fluence of >0.3 MWa/m^2, ITER will allow tests of tritium breeding module concepts and other fusion engineering components.

The harsh radiation environment near ITER resulting from this large DT neutron flux and the energetic gamma-rays created by neutron interactions in structures surrounding the plasma will create major challenges for plasma diagnostics on ITER. Neutron measurements provide important information on the physics behavior of tokamak plasmas [1]. This paper proposes novel applications of neutron activation techniques on ITER that should aid in the measurements of the total DT neutron production, the spatial profile of the neutron emission, and the energetic neutrons in the alpha knock-on tail above ~ 16 MeV resulting from collisions between the confined DT alpha particles and the fuel ions [2].

2.3. TOTAL NEUTRON PRODUCTION RATE

2.3.1. Background and Present Plans for ITER Neutron Activation Measurements

Measurements of the total number of DT neutrons produced in ITER will be used to determine the total fusion power output. Accurate measurements of the neutron output will play a fundamental role in determining the alpha particle heating, and hence in analyzing and understanding the physics of burning plasmas.

In addition, the total DT neutron production is a measure of the total amount of tritium burned in DT fusion reactions. ITER will routinely use large amounts of tritium as fuel, and

control of the tritium inventory will be a key operational issue both for environmental and safety reasons [3]. Given the uncertainty in the amounts of tritium that might be retained in the plasma-facing components, accurate and reliable measurements of the neutron production will be needed to calculate the amount of tritium that is unaccounted for and likely retained inside the vacuum vessel.

Neutron activation systems are planned on ITER to allow reliable measurements of the fusion power under all plasma conditions. The neutron flux integrated over the activation target exposure time should be measured with an accuracy of < 10%. ITER plans a conventional foil activation approach to neutron activation measurements [4]. Activation foil targets enclosed in transfer capsules will be pneumatically transferred to irradiation stations located near the plasma first wall where they are exposed to the ITER neutron flux for a measured time interval up to ~100 s. Following exposure, they will then be pneumatically transferred to a remote counting station, where the decay gamma rays resulting from neutron activation reactions can be measured. A detailed analysis using the Monte-Carlo neutron particle (MCNP) transport code will be used to establish the relationship between the total neutron production and the incident neutron fluence and energy spectrum at the target irradiation station locations.

Similar foil activation systems have been used for neutron flux measurements on present-generation tokamaks. The system presently planned for ITER is similar to those used on JET [5] and TFTR [6]. The higher neutron fluxes on ITER will allow the use of smaller activation targets and transfer capsules, and present plans call for the use of 9 mm diameter transport capsules on ITER [7] rather than the 25 mm diameter capsules employed on TFTR and JET. One significant difference on ITER will be that much of the transport line will not be accessible for maintenance and repairs as a result of the harsh radiation environment inside the biological shield. Transport capsules could sometimes get jammed or stuck inside the transport lines on JET and TFTR. If this should happen on ITER, it may be a very long time before personnel access is possible to repair the system. One approach might be to add several spare transport lines as backup systems for those times when a jammed capsule does block a transport line. ITER is also considering a remotely manipulated repair system where at several locations along the transport line, rods could be inserted to free a jammed transport capsule [8].

2.3.2 Proposed Neutron Activation System Using Gas Targets

We propose that a gas target activation system be installed on ITER in addition to the planned foil activation system. Gas targets are not often used for neutron activation measurements because signal levels are much higher in solid targets due to the significantly larger number of atoms of target material in a solid. But the very large neutron flux near the first wall of ITER will also allow the use of gas activation targets.

A schematic of a possible gas activation system for ITER is sketched in Fig. 1. The target gas at a known pressure would be released into a small (≤ 1 liter) exposure chamber just behind the ITER first wall by a small diameter gas feed line that could also be used to transfer the exposed gas back to a remote counting station. No moving parts would be required inside the biological shield; hence the system should be reliable and essentially failsafe. A typical target exposure cycle would consist of the following steps:

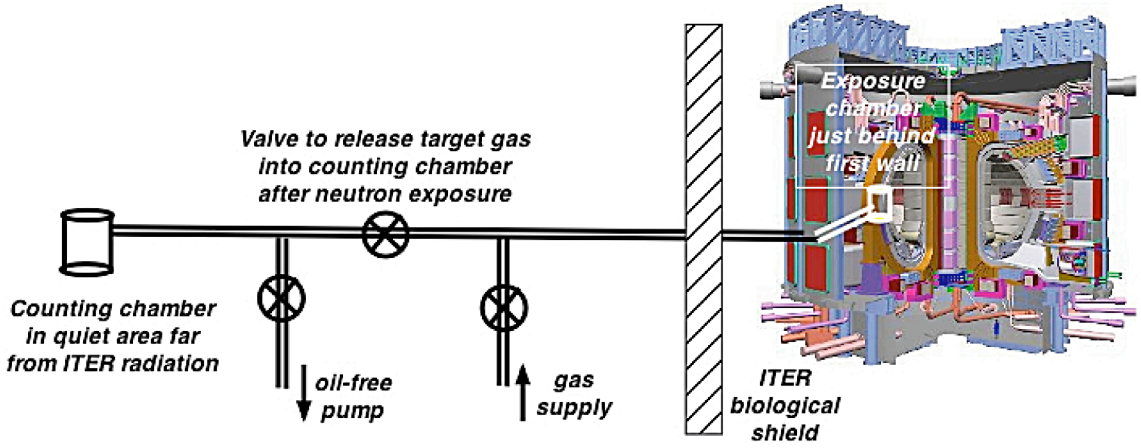

Fig. 1. Schematic of possible gas target neutron activation diagnostic on ITER.

1. Open the gas supply valve and fill the target exposure chamber with the selected target gas at the desired pressure set by the gas supply pressure regulator. Close the gas supply valve and measure the pressure in the target exposure chamber just prior to exposure to the neutrons from the plasma.
2. After the neutron exposure, open the inline valve connecting the exposure chamber to the counting chamber in the remote quiet/counting area. The activated gas would redistribute with a known fraction ending up in the counting chamber, determined by the ratio of the counting chamber volume to the total volume of the counting chamber, exposure chamber and the gas feed line (corrected for any temperature differences).
3. Measure the activation decay gammas from the portion of the activated gas contained in the counting chamber.
4. Open the pump valve and remove the activated gas from both chambers and the gas feed line in preparation for the next target exposure.

Several gas target activation reactions that appear suitable for DT neutron yield measurements are listed in Table 1. Using noble gases is attractive since they are not a safety issue for either the tokamak or personnel. We also show a nitrogen and an oxygen reaction that could be used. The list in Table 1 is far from complete, e.g. there are many additional

Table 1
Some Candidate Reactions for Measuring DT Neutron Production on ITER Using a Gas Activation System

Target Reaction	Threshold Energy (MeV)	Cross-Section at 14 MeV (mBarns)	Half-Life of Decay	Decay Mode	Gamma Decay Energies (MeV)
Ne^{22} (n, α) O^{19}	6.0	22	29.4 s	β^-	0.197 1.36
Ar^{40} (n, d) Cl^{39}	10.6	1.3	56 min	β^-	1.27 0.26
Kr^{86} (n, 2n) Kr^{85m}	10.0	1,130	4.4 h	IT, β^-	0.15 0.30
Xe^{136} (n, 2n) Xe^{135m}	8.1	860	15 min	IT	0.53
N^{14} (n, 2n) N^{13}	10.6	6	10 min	β^+	0.511
O^{16} (n, p) N^{16}	10.2	44	7.1 s	β^-	6.13 7.12

reactions of interest for krypton and xenon, both of which have several isotopes as natural constituents. A one liter target exposure chamber (EC) filled to a pressure of one atmosphere contains $\sim 3 \cdot 10^{22}$ target atoms of gas. For an ITER plasma producing 500 MW of fusion power, the neutron flux at the first wall will be $\sim 2.6 \cdot 10^{13}$ n/cm^2/s. After a 10 s exposure to neutrons at the first wall of ITER, an Argon target with an activation cross-section of 1.3 mbarn at 14 MeV would result in $\sim 9 \cdot 10^9$ total activated atoms, and an initial decay rate of $\sim 1.9 \cdot 10^6$/s. After opening the inline valve in Fig. 1, the fraction of this activated gas that ends up in a 2 liter counting chamber (CC) would be $f = V_{CC} / (V_{EC} + V_{CC} + V_{GL})$, where V_{GL} is the volume of the gas line connecting the two chambers. The time scale for the exposed gas to equilibrate into the counting chamber is $\tau = V_{CC} / C$, where C is the conductance of the the gas line. For $V_{GL} \sim V_{CC}$, $\tau \sim 45$ s. Using a high purity Ge(Li) detector and a 2 liter "Marinelli beaker" shaped gas container, we could detect ~ 3 % of the 0.26 MeV decay gammas emitted by the activated gas in the Marinelli beaker [9]. Hence, the detected gamma rate should be $\sim 1.6 \cdot 10^4$/s. This is near the expected upper limit of the gamma energy spectrometer electronics, which is limited by the desired energy resolution and pulse pile-up effects [10]. This signal counting rate should result in more than adequate statistics, contributing only ~ 1% to the error in the neutron flux measurements even for very short-lived (half-life ~ 1 s) activation decays.

Gas activation reactions with significantly larger cross-sections or shorter decay product half-lives would require reducing either the neutron exposure time and/or the exposure

chamber gas fill pressure to avoid non-linear/saturation effects in the pulse height analysis electronics of the gamma-ray energy spectrometer.

Adding a gas target neutron activation system on ITER in addition to the planned foil activation system would have several advantages:

a. Since no transport capsules are required in a gas activation system, there would be no possibility of a jammed or stuck transport capsule…. making it essentially failsafe.

b. Avoid the need to use a remote manipulator to remove the target from the transport capsule prior to counting the decay gammas, as is likely to be required for the foil activation system.

c. The gas pressure used to fill the exposure chamber can be chosen to optimize the expected decay signal counting rate based on the expected plasma neutron flux and target exposure time.

d. Decay signal counting rate can also be optimized after the shot to the maximum rate allowed by the detection electronics by reducing the pressure of the exposed gas inside the counting chamber.

2.4. SPATIAL PROFILES OF THE NEUTRON EMISSION

2.4.1. Background and Present Plans for Neutron Cameras on ITER

Measurements of the spatial profile of the neutron emission per unit volume in ITER are needed to determine the alpha particle birth profile. The birth profile will be used in calculating the spatial profile of the alpha particle heating, and will be important to analyzing and understanding the physics of burning plasmas. The neutron emission profile data will also improve the accuracy in the measurement of the total neutron production rate.

As shown in Fig. 2, a radial neutron camera (RNC) and a proposed vertical neutron camera (VNC) have been designed to measure the neutron emission profile on ITER. The length of the ITER equatorial port limits the view of the RNC detectors that are located outside the vacuum vessel so that this ex-vessel RNC will only measure the central core region of the plasma ($-0.5 < r/a < 0.5$). Measurements outside this core region will rely on views of the plasma edge provided by additional compact in-vessel collimators and detectors (labeled Compact RNC) in Fig. 2. With these additional edge channels, the "extended" RNC can measure the neutron emission profile from $-0.9 < r/a < 0.9$. The fraction of the neutrons produced outside $r/a \sim 0.5$ and only seen by these in-vessel RNC detectors can be as large as 10–20%. The need for a VNC in addition to a RNC is based on recent JET results, which show that the neutron emission profile is not constant on a plasma flux surface during ICRF heating, neutral beam injection, sawtooth oscillations, Alfven eigenmodes, and other instabilities [11].

The in-vessel detectors of the Compact RNC and the VNC are inside the biological shield where access for maintenance and detector replacement will be very restricted. The high neutron and gamma ray fluences can cause radiation damage to the neutron detectors, and only the most robust and radiation resistant detectors are under consideration for these locations. Similar concerns exist for the ex vessel RNC, although access to these detectors should be less restricted. Among the detectors being considered for the in vessel neutron cameras are ^{238}U fission chambers, scintillators, and diamond detectors. ^{238}U fission chambers have superior radiation resistance, but will have difficulty in achieving the microsecond time response needed for studying MHD instabilities. Scintillators will also be sensitive to gamma rays, and neutron damage can cause browning and reduce their light output. Natural diamond detectors begin to exhibit a drop in their charge collection efficiency (CCE) after exposure to a fast neutron fluence of ~ 10^{14} n/cm^2 [12], expected to occur after only 3 to 4 months of operation during the initial phase of DT experiments.

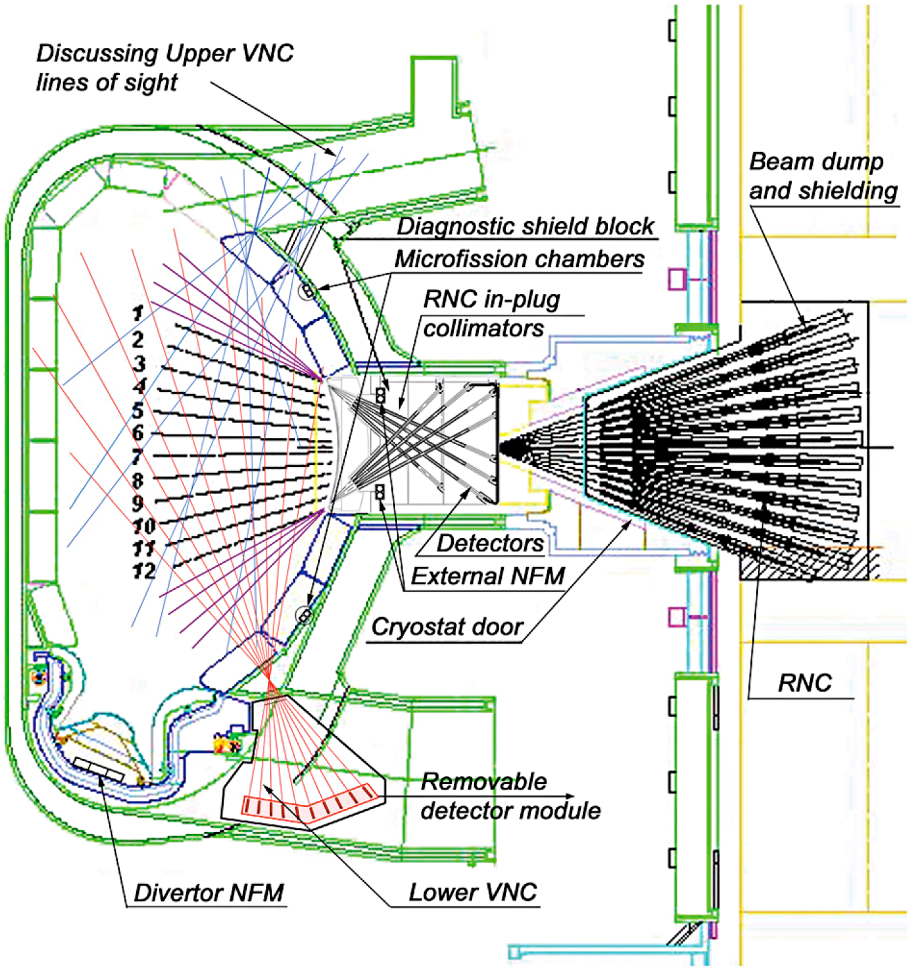

Fig. 2. Arrangement of radial neutron camera (RNC and RNC in-plug collimators and detectors) and two possible vertical neutron camera (VNC) designs for ITER. [Reproduced from A.V. Krasilnikov, et al., Nucl. Fusion **45**, 1503 (2005) Copyright © Institute of Physics and IOP Publishing Limited 2009.]

Plans for the absolute calibration of all of the ITER neutron diagnostics, including the detectors in the RNC and VNC, are being developed [13]. This includes absolute calibration of all neutron detectors at the manufacturer, and calibration at ITER in a purpose-built onsite laboratory. ITER also plans an *in situ* calibration of the neutron diagnostics using neutron sources located inside the vacuum vessel. Calibration data for the detectors designed to measure the total neutron production will be taken with the neutron source located at the plasma axis where the ion temperature and hence the neutron production is typically largest. This neutron source will be moved toroidally around the vacuum vessel on a track similar to a model railroad system. Data with the neutron calibration source at off-axis locations will provide better information on the effect of the plasma neutron emission profile as a function of (r,θ) in the poloidal plane. The calibration source is expected to be a DT neutron generator producing $\leq 10^{11}$ n/s, and/or a radionuclide source.

Calibration of the neutron camera detectors will require measurements with the neutron source at least several of the off-axis locations inside the plasma volume viewed by the spatial channels of the RNC and VNC. This approach will allow a) checking the detection efficiency and the viewing volume of the collimated neutron detectors, and b) checking the cross-talk between different spatial channels of the neutron camera that results from neutron scattering and/or leakage transmission through the neutron collimators. The *in situ* calibration with the neutron source inside the ITER vessel is expected to require up to several weeks. The most suitable time is likely to be at the end of the hydrogen phase of ITER operations, when much of the hardware that can scatter neutrons and hence affect the calibration will already be installed.

Since the calibration source will produce several orders of magnitude fewer neutrons/ second than high power DT plasmas, only the most sensitive detectors in the installed neutron diagnostics can be absolutely calibrated in this manner. Extrapolating the absolute calibration to the less sensitive detectors, that will actually be used to measure the fusion output power, will involve a cross calibration using the plasma as the neutron source.

2.4.2. Proposed Addition of Neutron Activation Detectors to the ITER Neutron Cameras

We propose that a spatial array of foil activation detectors be added to the ITER RNC. Irradiation stations for activation targets would be installed at locations adjacent to each of the neutron detectors in both the Compact RNC and the ex-vessel RNC. An activation detector would view the plasma through the same neutron collimator used by each of the present neutron camera detectors. The addition of these activation detectors would have several objectives and advantages:

1. Given the highly restricted access to the neutron detectors in the Compact RNC, it will not be possible to immediately replace any of the time-resolved neutron detectors

that should fail. ITER plasma operations are likely to continue for several weeks or even months before repairs may be possible. Replacement of any failed detectors in the ex-vessel RNC will be also be limited by access restrictions. While not capable of millisecond time resolution, the proposed foil activation detector array would allow neutron profile measurements integrated over the neutron exposure time for the activation target, which could be as short as a second or less. This would ensure that neutron emission profile data would continue to be available until the time-resolved detectors that had failed could be replaced.

2. Adding activation detectors to the neutron camera detector arrays would allow comparisons with the emission profile measured using the camera's time-resolved neutron detectors. This would help uncover any changes in the response of the time-resolved detectors due to radiation damage, and should also aid in determining whether any observed changes in the time-resolved signals are due to changes or misalignments in the neutron collimator performance. This would allow faster determination of whether any observed changes in the spatial profiles of the measured signals are due to changes in the plasma neutron source profile or due to changes in either in the detector response or the collimator performance.

3. The activation detectors should also aid in maintaining the absolute calibration of the time-resolved neutron camera detectors. Radiation damage can cause detectors in the neutron cameras to fail. When these failed detectors are replaced, the replacement detectors are unlikely to all have the same absolute detection efficiency or response. By comparing the neutron emission profile of a "standard shot" or reference plasma measured using the newly installed time-resolved detectors with that measured by the activation detectors, it should be possible to use the activation detector data as a calibration reference, both in terms of the relative channel-to-channel calibration, and the absolute signal level calibration.

2.5. MEASUREMENTS OF THE ALPHA KNOCK-ON TAIL

2.5.1. Background and ITER Plans

For DT magnetic fusion to be useful for energy production, it is essential that the energetic alpha particles produced by the fusion reactions be confined long enough to deposit a significant fraction of their initial ~ 3.5 MeV energy in the plasma before they are lost. Development of diagnostics to study the behavior of energetic confined alpha particles is a very important if not essential part of burning plasma research**.** Despite the clear need for these measurements, development of diagnostics to study the fast confined alphas to date has proven extremely difficult, and the available techniques remain for the most part unproven and with significant uncertainties.

Collective Thomson scattering is the only technique that appears to be capable of measuring the temporal and spatial profile of the fast confined alpha particle energy distribution, and as such is the mainline approach to alpha diagnostics [14]. The recent results on TEXTOR and ASDEX-U are encouraging, but there remain uncertainties in its implementation and interpretation on ITER. Pellet charge exchange, used to obtain the first measurements of the energy and spatial profiles of fast confined DT alphas in experiments [15] on TFTR, would be limited by pellet penetration to measurements outside r/a ~ 0.5 in ITER.

Information on the confined alpha particles can also be obtained from measurements of the neutron and ion tails resulting from alpha particle knock-on collisions with the plasma deuterium and tritium fuel ions [16]. One of the strengths of this approach is the ability to measure the alphas in the hot plasma core where the interesting ignition physics will occur.

The fraction of neutrons in the knock-on tail is only 10^{-4} to 10^{-3} of the total DT neutrons, which makes their measurement very difficult. Conventional techniques such as pulse height spectroscopy and time-of-flight are not suitable for knock-on measurements due to the number of false signal events expected at total counting rates large enough for useful observations of the knock-on tail. The alpha knock-on tail has been experimentally observed using a large magnetic proton recoil (MPR) spectrometer during DT experiments on JET [17]. The small knock-on signal levels in the MPR limited the information available about the behavior of the alphas in JET. Due to its relatively low neutron detection efficiency, the MPR would have to be closely coupled to ITER in order to increase the incident neutron flux arriving at the MPR. This is necessary to improve the neutron counting statistics and allow alpha particle physics studies, but will be very difficult given the diagnostics port and space constraints on ITER.

2.5.2. Proposed Measurements of the Alpha Knock-On Tail Using Neutron Activation

We propose to measurement the alpha knock-on neutron tail on ITER using activation detectors with neutron energy thresholds > 15.5 MeV. This approach looks attractive for several reasons:

1. Activation targets with different threshold energies between 15.5 and 20 MeV would allow measurements of the knock-on tail neutron energy spectrum, yielding information on the energy spectrum of the confined alpha particles in the plasma.
2. The targets can be exposed to the very high neutron flux near the first wall of ITER, increasing the knock-on signal levels and the counting statistics.
3. After exposure, the activation targets will be transferred to a counting room, where the activation decay signals will be measured after the tokamak discharge and in a low radiation background environment.

4. Experimental measurements of the activation cross-sections as a function of the incident neutron energy allow calculation of the detector response.
5. Neutron activation techniques are inherently a very reliable and robust approach, well suited to the ITER hostile environment for diagnostics.
6. Knock-on measurements using activation, while not capable of the temporal and spatial profile information provided by collective scattering, would provide a valuable check on the collective scattering results as well as serve as a reliable backup diagnostic when collective scattering data is unavailable.

There are two principal disadvantages of the activation approach:

1. Time resolution will be very limited since the results are integrated over the target exposure time. Depending on the activation target, the exposure time is expected to be at least a fraction of a second, and may often be tens of seconds or longer.
2. Measurements of the activation decays will often take several hours, delaying the availability of the results until long after the plasma exposure.

Figure 3 shows the calculated knock-on neutron tail spectrum [18] for a DT plasma with T_e= 20 keV and $n_e = n_i = 5 \cdot 10^{13}$ cm^{-3}, comparable to the conditions expected in ITER. The knock-on spectrum becomes larger than the thermonuclear and beam-target neutron distributions at energies $E_c > 15.5$ MeV. The alpha particles are assumed to be well confined, i.e. they are confined for a time that is long compared to their slowing-down time. Hence they deposit a large fraction of their initial energy into the plasma before they are lost. Under these conditions, Fig. 3 shows that the amplitude of the knock-on tail falls with neutron energy E_n as exp $\{- E_n / kT_{tail})$ where $kT_{tail} \sim 0.44$ MeV. For each 1.0 MeV increase in the neutron energy, the fraction of knock-on neutrons above that energy falls by ~ a factor of 10.

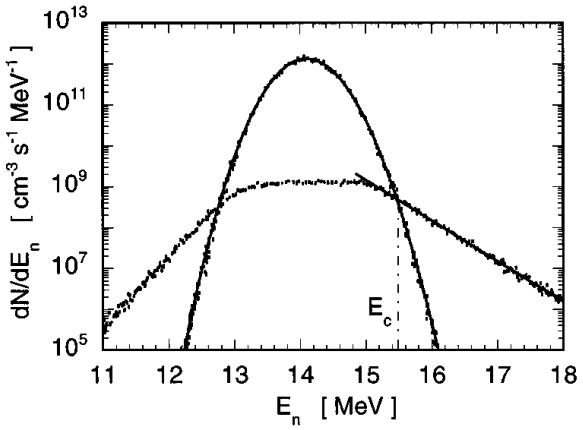

Fig. 3. Calculated neutron spectrum from a DT plasma with T_e= 20 keV and $n_e = n_i = 5 \cdot 10^{13}$ cm^{-3}, comparable to the conditions expected in ITER. [Reproduced from L. Ballabio, et al., Phys. Rev. E **55**, 3358–3368 (1997).]

Measurements of the size and shape of the knock-on neutron energy spectrum between 15.5 and 20 MeV will yield information on the confinement of the confined alphas in ITER. The lower energy portion of the neutron tail near 15.5 MeV requires fuel ion energies ≥250 keV, which depending on the scattering angle in the alpha-fuel ion collisions, can result from alphas with energies anywhere between ~250 keV and the alpha particle birth energy. The highest energy portion of the knock-on tail near ~ 20 MeV, on the other hand, can only result from alphas near their birth energy. Equivalently, alphas near their birth energy will contribute neutrons over the entire range of 15.5 to 20 MeV, while lower energy alphas can only contribute to the lower energy portions of the knock-on tail. If the alpha confinement deteriorates as a result of slow or diffusive-type losses, fewer alphas will survive to reach lower alpha energies. Without the contribution of these lower energy alphas to the knock-on fuel ion tails, the net effect of the deterioration in the alpha confinement will be to reduce the lower energy portion of the knock-on neutron tail. Any rapid alpha loss such as first orbit losses or toroidal field ripple losses that affect the birth energy alphas will suppress the size of the neutron tail, but not affect the shape. By measuring the knock-on spectrum using activation detectors with several energy thresholds between ~15.5 and 20 MeV, we can hope to obtain information on both the size and shape of the knock-on tail.

A recent study has examined the effects of the ICRF heating and the MeV deuterium neutral beams planned for plasma heating and current drive on the ITER neutron emission spectrum [19]. The resulting fast ions react with the thermal fuel ions, producing energetic neutrons that can interfere with observation of the alpha knock-on tail. Beam target neutrons resulting from the MeV beam ions interacting with the thermal plasma ions dominate the neutron emission between ~15 and 16.7 MeV for neutrons emitted in the same toroidal direction as the beam injection. Observing the alpha knock-on tail would then require observing neutron with energies > 16.7 MeV. A second possibility would be to observe neutrons emitted in the opposite toroidal direction from the beam injection, so that the neutron energy would be decreased as a result of the excess energy in the center of mass system.

Table 2 lists several candidate activation reactions with neutron energy thresholds above 15.5 MeV.

To determine if a given reaction will be useful, we need to calculate the expected size of the signal due to the alpha knock-on tail, as well as the size of the competing background signals resulting from other neutron-induced reactions that might occur in the target. Activation decays resulting from the much larger DT neutron flux near 14 MeV reacting with any of the isotopes of the target material, or with impurities in the target, can result in decay gamma emission that would prevent observation of the knock-on tail signal. All possible reactions including (n,2n), (n,3n), (n,p), (n,d), (n,t), (n,^{3}He), (n,α), (n,n'), (n,n+p), (n,n+d), (n,n+t), and (n, n+α) reactions must be examined. Given the small fraction (10^{-4} to 10^{-3}) of

the total DT neutron flux in the alpha knock-on tail, and the large number of background reactions, finding suitable targets requires careful analysis. This analysis has not been completed for all of the reactions in Table 2. Signal reactions resulting in decay products with decay half-lives longer than the competing background decays are attractive, since the knock-on signal can be observed after the much larger background signals have decayed away. More details on three activation reactions that appear promising are discussed below.

Table 2
Some Neutron Activation Reactions with
Threshold Energies E_{th} > 15.5 MeV

Target Reaction	Threshold Energy (MeV)	Half-Life of Decay	Decay Mode	Gamma Decay Energies
S^{32} (n, 2n) S^{31}	15.52	2.6 s	β^+	0.511 MeV
Ne^{20} (n, t) F^{18}	15.54	110 min	β^+, EC	0.511 MeV
Ca^{40} (n, 2n) Ca^{39}	16.0	0.86 s	β^+	0.511 MeV
Be^9 (n, d) Li^8	16.31	0.84 s	β^-	~13 MeV β^- directly
O^{16} (n, 2n) O^{15}	16.65	2 min	β^+	0.511 MeV
La^{138} (n, 3n) La^{136}	16.75	9.5 min	EC, β^+	0.511, 0.83, 1.32, 2.1 MeV
Mg^{24} (n, 2n) Mg^{23}	17.2	11.3 s	β^+	0.511 MeV
Pr^{141} (n, 3n) Pr^{139}	17.46	4.5 h	EC, β^+	1.35, 1.63 MeV
Ne^{20} (n, 2p) O^{19}	17.74	27 s	β^+, EC	0.2, 1.55, 2.6, 4.2 MeV
Si^{28} (n, 2n) Si^{27}	17.8	4.1 s	β^+	0.511 MeV
C^{12} (n, 2n) C^{11}	20.3	20.4 min	β^+, EC	0.511 MeV

2.5.2.1. Ne^{20} (n, t) F^{18} Reactions. This reaction has a neutron energy threshold of 15.54 MeV. The resulting F^{18} decays via positron emission with a half-life of ~ 110 minutes. While gases are not normally used in neutron activation measurements due to their low target density, the combination of a very attractive threshold for knock-on measurements and a long decay time make this reaction of interest. A one liter gas target exposure chamber installed just behind the first wall on ITER filled with 100 atmospheres of neon gas would contain $N_{target} \sim 2.4 \cdot 10^{24}$ of Ne^{20} atoms.

The expected decay signal dN_{decay}/dt from an activation target containing N_{target} atoms of Ne^{20} and exposed to a neutron fluence of Φ_n is

$$dN_{decay}/dt = N_{target}\, \sigma_{eff}\, f_{K\text{-}O}\, \Phi_n / \tau_{decay} \quad ,$$

where $\sigma_{eff}\, f_{K\text{-}O} = \int df_{K\text{-}O}(E)/dE\, \sigma(E)\, dE \cong 1.2 \cdot 10^{-9}$ barns, where $df_{K\text{-}O}/dE$ is the fraction of the total DT neutrons in the knock-on neutron tail, and $\sigma_{n,t}(E)$ is the Ne^{20}(n, t) activation cross-section. After a 100 s exposure in ITER at the $2.4 \cdot 10^{13}$ n/cm^2-s flux location discussed earlier,

there would be ~$7 \cdot 10^6$ total signal activations, resulting in ~1,500 positron decays/second. Approximately 1% of the coincident 511 keV gamma decays could be detected using two 3 in. diameter by 3 in. thick Na(I) scintillators, one on each face of a 3 in. diameter by 2 in. long "counting" chamber. Hence, the detected coincident gamma rate should be ~15/s. For comparison, the measured background on a similar coincident gamma decay detector used at the OMEGA inertial confinement fusion experiment was only ~ $5 \cdot 10^{-3}$/s [20]. The Na(I) detectors were shielded with 7.6 cm of lead to reduce the background due to cosmic rays. The coincident detectors were located 120 m from the target plasma to isolate the detectors from direct activation by the DT neutrons from the OMEGA plasma.

The much larger flux of DT neutrons near 14 MeV incident on the neon target at ITER would result in a very large background of 1.63 MeV gamma-rays due to Ne^{20} (n, p) F^{20} reactions in the neon gas, but F^{20} decays with a half-life of only 11 s, so that this background should become negligible ~ 7 minutes after the end of the exposure to the plasma neutrons, allowing the longer-lived signal due to the Ne^{20} (n, t) F^{18} reactions resulting from the alpha knock-on neutrons to be measured.

High purity neon gas must be used for the activation target, but is fortunately available in the required purity. For example, research grade neon from Spectra Gases has < 1 part per million (ppm) of N_2, and even higher purities are available. At 1 ppm of nitrogen, the background decay rate from N^{14}(n, 2n) N^{13} reactions would initially be ~ 6 times larger than the signal. N^{13} decays via positron emission, and hence will result in coincident 511 keV gammas, just as the knock-on signal does. But the N^{14}(n, 2n) N^{13} background gammas would decay away with a 10 minute half-life. Within 30 minutes after exposure, the 110 minute half-life Ne^{20}(n, t) activation signal would begin to appear. Any other background radiation due to impurities in the neon gas can also be expected to have a significantly shorter decay time, allowing the knock-on signal from the Ne^{20}(n, t) decays to be counted.

2.5.2.2. Pr^{141} (n, 3n) Pr^{139} Reactions. This reaction has a neutron energy threshold of 17.46 MeV, and hence would provide a second data point on the measured knock-on neutron energy spectrum. Praseodymium is a rare earth metal that can be used in a solid target pneumatic transport system. The resulting Pr^{139} decays via positron emission with a half-life of ~ 4.4 h. A 100 gm Pr target would contain $N_{target} \sim 4.3 \cdot 10^{23}$ of Pr^{141} atoms. For Pr^{141}(n, 3n) activation, $\sigma_{eff} f_{K\text{-}O} = \int df_{K\text{-}O}(E)/dE\ \sigma(E)\ dE \cong 9 \cdot 10^{-9}$ barns, where $df_{K\text{-}O}/dE$ is the fraction of the total DT neutrons in the knock-on neutron tail, and $\sigma_{n,t}(E)$ is the activation cross-section. After a 100 s exposure in ITER at the $2.4 \cdot 10^{13}$ n/cm^2-s flux location, there would be ~$9.3 \cdot 10^6$ total signal activations, with 7.9% of these or ~740,000 of these decaying via positron emission, and resulting in ~46 positron decays/second. Approximately 4% of the coincident 511 keV gamma decays from the positron decays could be detected using the coincident gamma detector geometry described earlier. Hence, the total number of detected coincident gamma decays would be ~ 30,000 and the initial detected decay rate would be ~ 1.8/s.

There will be a number of competing background reactions due to the large flux of DT neutrons near 14 MeV interacting with the Praesydium target. $Pr^{141}(n, 2n)Pr^{140}$ reactions would result in a large background of 0.511 KeV gammas but this background has a half-life of only 3.4 min and would be negligible ~ 2 hrs after the exposure. $Pr^{141}(n,p)$ Ce^{141} reactions would result in a large background of 0.144 MeV gammas with a half-life of 32 days. But coincident detection techniques could be used to discriminate against this background and allow observation of the alpha knock-on signal gammas.

2.5.2.3. La^{138} (n, 3n) La^{136} Reactions. This reaction has a neutron energy threshold of 16.75 MeV, and hence would provide a third data point on the measured knock-on neutron energy spectrum. Lanthanum is also a rare earth metal that can be used in a solid target pneumatic transport system. The resulting La^{136} decays via positron emission with a half-life of ~ 9.5 minutes. A 100 gm La target would contain $N_{target} \sim 3.9 \cdot 10^{20}$ of La^{138} atoms. For La^{138}(n, 3n) activation, $\sigma_{eff} f_{K\text{-}O} \cong 1.3 \cdot 10^{-7}$ barns. After a 100 s exposure in ITER at $2.4 \cdot 10^{13}$ n/cm^2-s, there would be $\sim 1.2 \cdot 10^5$ total signal activations, with 33% of these or ~40,000 of these decaying via positron emission, and resulting in ~48 positron decays/second. Approximately 4% of the coincident 511 keV gamma decays from the positron decays could be detected using the coincident gamma detector geometry described earlier. Hence, the total number of detected coincident gamma decays would be ~ 1600 and the initial detected decay rate would be ~ 1.9/s.

There will be a number of competing background reactions due to the large flux of DT neutrons near 14 MeV interacting with the Lanthanum target. $La^{139}(n, p)Ba^{139}$ reactions will result in a large background of 0.166 MeV gammas with a half-life of 83 min. $La^{139}(n,\alpha)$ Cs^{136} reactions will result in a large background of 1.04 MeV gammas with a half-life of 13 days. But coincident detection techniques can be used to discriminate against both of these backgrounds and should allow observation of the alpha knock-on signal.

2.5.2.4. Other Reactions, Radiochemistry. Future research should include examining each of the other reactions shown in Table 1 in more detail, with the goal of deciding which reactions should be most useful for alpha knock-on measurements. There are likely also other candidate reactions of interest that are not yet identified and listed in Table 1. My optimism is based on the fact that in my earlier research on finding suitable threshold activation reactions, I did not take into account the possibility of using radiochemistry techniques to reduce or remove the problematic backgrounds. For example if an (n,2n) reaction produced the signal, but was competing with larger backgrounds from (n,p), (n,d), (n,t) or (n,α) reactions, the background reactions would all result in an end product that is a different element i.e. with a atomic charge Z that is smaller than the Z of the signal decay element. Hence chemistry could be hopefully be used to separate the decay signal from the background sources.

2.6. SUMMARY

Novel applications of neutron activation techniques are proposed to aid in the measurements of the total DT neutron production, the spatial profile of the neutron emission, and the energetic neutrons above ~ 16 MeV resulting from DT alpha particle collisions with fuel ions on ITER.

REFERENCES

[1] Jarvis, O.N., Plasma Phys. and Controlled Fusion **36**, 209 (1994).

[2] Fisher, R.K., et al., Nucl. Fusion **34**, 1291 (1994); G. Gorini, et al., Rev. Sci. Instrum. **66**, 936 (1995).

[3] Loire, A., et al., ITER Physics Basis, Ch.4 Power and particle control, Nucl. Fusion **47**, S223 (2007).

[4] Barnes, C.W., et al., Rev. Sci. Instrum. **68,** 577 (1997).

[5] Jarvis, O.N., et al., Fusion Technol. **20,** 265 (1991).

[6] Barnes, C.W., et al., Rev. Sci. Instrum. **66,** 888 (1995).

[7] Walker, C.I., "Activation System for Neutron Diagnostics," ITER Report ITER_D_223ESD (2005).

[8] Bertalot, L., private communication, October 2007.

[9] ORTEC, "The Best Choice of High Purity Germanium (HPGe) Detector," Fig. 12, p.7 available at www.ortec-online.com

[10] ORTEC, "The Best Choice of High Purity Germanium (HPGe) Detector," Fig. 17, p.10 available at www.ortec-online.com

[11] Popovichev, S., et al. "Neutron Emission Profile and Neuron Spectrum Measurements at JET: Status and Plans," Proc. 2007 Varenna Conf. on Burning Plasma Diagnostics, AIP Conf. Proc. **988**, 275 (2008).

[12] Krasilnikov, A.V., et al., Nucl. Fusion **45**, 1503 (2005).

[13] Petrizzi, L., et al., 8th ITPA Meeting of Diagnostic Topical Group, Culham, 14-18 Mar 2005: and Kauchek, Varenna 2007.

[14] Meo, F., et al., Rev. Sci. Instrum. **75**, 3585 (2004).

[15] Fisher, R.K., et al., Phys. Rev. Lett. **75**, 846 (1995).

[16] Fisher, R.K., P.B. Parks, J.M. McChesney and M.N. Rosenbluth, Nucl. Fusion **34**, 1291 (1994); and Gorini, G. L. Ballabio, and J. Källne, Rev. Sci. Instrum. **66**, 936 (1995).

[17] Kallne, J., et al., Phys. Rev. Lett. **85**, 1246 (2000).

[18] Ballabio, L., et al., Phys. Rev. E **55**, 3358-3368 (1997).

[19] Eriksson, L.-G., "The effect of RF- and NBI-driven fast ions in ITER on various diagnostics," presented by L. Bertalot at the 13th Meeting of the ITPA Topical Group on Diagnostics, Chengdu, PRC, Oct 29–Nov 2, 2007.

[20] Glebov, V. Yu., et al., Rev. Sci. Instrum. **74**, 1717 (2003).

ACKNOWLEDGEMENT

This research was supported by U.S. Department of Energy Grant DE-FG02-92ER54150.